

- SPEK, A. L. (1983). Proc. 8th Eur. Crystallogr. Meeting, Belgium.
- WIEGERS, G. A. & MEERSCHAUT, A. (1992). In *Incommensurate Sandwiched Layered Compounds*, edited by A. MEERSCHAUT, pp. 101–172. Trans. Tech. Pub.
- WIEGERS, G. A., MEETSMA, A., VAN SMAALEN, S., HAANGE, R. J. & DE BOER, J. L. (1990). *Solid State Commun.* **75**, 689–692.
- WIEGERS, G. A., MEETSMA, A., VAN SMAALEN, S., HAANGE, R. J., WULFF, J., ZEINSTR, T., DE BOER, J. L., KUYPERS, S., VAN TENDELOO, G., VAN LANDUYT, J., AMELINCKX, S., MEERSCHAUT, A., RABU, P. & ROUXEL, J. (1989). *Solid State Commun.* **70**, 409–413.
- ZHOU, W. Y., MEETSMA, A., DE BOER, J. L. & WIEGERS, G. A. (1992). *Mat. Res. Bull.* **27**, 563–572.

Acta Cryst. (1995). **B51**, 287–293

Structure of Potassium Sulfate at Temperatures From 296 K Down to 15 K

BY KENJI OJIMA, YASUO NISHIHATA AND AKIKATSU SAWADA

Faculty of Science, Okayama University, Okayama 700, Japan

(Received 18 July 1994; accepted 18 November 1994)

Abstract

The crystal structure of potassium sulfate, K_2SO_4 , was studied at five temperatures from 296 down to 15 K using an off-center four-circle diffractometer. The temperature dependence of lattice constants is well explained by the Grüneisen relation. The crystal structure is confirmed to be orthorhombic, space group $Pm\bar{c}n$, down to 15 K. The S—O bond lengths in SO_4 tetrahedra with thermal motion correction are almost independent of temperature. Atomic positions of K(1), K(2) and S atoms in the β - K_2SO_4 structure are found to approach the special positions in the α - K_2SO_4 structure as temperature increases. No evidence for any phase transition has been detected below room temperature.

Introduction

Many compounds of A_2BX_4 -type crystals have the β - K_2SO_4 -type structure and some of these compounds have interesting features. For example, ammonium sulfate, $(NH_4)_2SO_4$, shows ferroelectric temperature dependence on spontaneous polarization (Unruh, 1970). Potassium selenate, K_2SeO_4 , transforms into an incommensurately modulated phase (Iizumi, Axe & Shirane, 1977). Tetramethylammonium tetrabromocobaltate and tetramethylammonium tetrabromozincate, $[N(CH_3)_4]_2XBr_4$ ($X = Zn, Co$), show ferrielastic temperature dependence on monoclinic angle deviation from 90° below T_c (Hasebe, Mashiyama, Tanisaki & Gesi, 1984; Sawada, Tanaka, Matsumoto & Nishihata, 1995). Potassium sulfate, K_2SO_4 , is the most fundamental crystal among the β - K_2SO_4 -type crystals. Lattice constants and positional parameters at room temperature were reported by Robinson (1958) and later refined by McGinnety (1972). This crystal undergoes a first-order phase transition from the β - (orthorhombic, space group $Pm\bar{c}n$) to the α - K_2SO_4 structure (hexagonal, space group $P6_3/mmc$) at high temperature. El-Kabbany

(1980) reported a hysteresis with a transition temperature of 844 K on heating and 839 K on cooling. High-temperature study of the structure has been reported by van den Berg & Tuinstra (1978), Miyake, Morikawa & Iwai (1980), and Arnold, Kurtz, Richter-Zinnius, Bethke & Heger (1981). On the other hand, it was suggested from measurements of specific heat and dielectric constants that K_2SO_4 might undergo another phase transition at 56 K (Gesi, Tominaga & Urabe, 1982). The crystal structure of potassium sulfate below room temperature has not yet been reported.

The purpose of the present work is to study the crystal structure of potassium sulfate by single-crystal X-ray diffraction in the temperature range from room temperature down to 15 K. In particular, we examine whether such a phase transition really occurs.

Experiment

Single crystals of potassium sulfate were grown by slow evaporation of an aqueous solution. Integrated intensity data were measured using an off-center-type four-circle diffractometer with a χ -cradle of inner diameter 400 mm (Huber Eulerian cradle model 512), installed in the X-ray Laboratory of Okayama University. Graphite monochromatized Mo $K\alpha$ radiation was used. The shape and size of the crystal used during the experiments was spherical, diameter 0.298 (2) mm at 296, 50 and 15 K and 0.265 (2) mm at 200 and 100 K. The specimen attached to a sapphire rod was cooled by a closed-cycle helium gas refrigerator which was mounted on the φ -circle of the diffractometer. The temperature was measured by a thermocouple, Au(Fe)-chromel, attached on the supporting rod apart from the specimen by *ca* 1.5 mm. Temperature stability during the experiments was within ± 0.5 at 296, 50 and 15 K, and also within ± 1.0 at 200 and 100 K. Lattice parameters were refined

Table 1. Crystallographic data and experimental details

Crystal data	296	200	100	50	15
Temperature (K)					
Crystal system	Orthorhombic	Orthorhombic	Orthorhombic	Orthorhombic	Orthorhombic
Space group	<i>Pm</i> <i>cn</i>	<i>Pm</i> <i>cn</i>	<i>Pm</i> <i>cn</i>	<i>Pm</i> <i>cn</i>	<i>Pm</i> <i>cn</i>
<i>a</i> (Å)	5.7704 (3)	5.7503 (4)	5.7303 (6)	5.7224 (5)	5.7226 (4)
<i>b</i> (Å)	10.0712 (9)	10.0395 (6)	10.010 (1)	10.000 (1)	9.9985 (4)
<i>c</i> (Å)	7.4776 (4)	7.4513 (7)	7.4291 (6)	7.4226 (6)	7.4218 (4)
<i>V</i> (Å ³)	434.56 (5)	430.16 (5)	426.14 (7)	424.73 (7)	424.66 (4)
<i>Z</i>	4	4	4	4	4
Density (g cm ⁻³)	2.66	2.69	2.72	2.73	2.73
Radiation	Mo <i>K</i> α ₁	Mo <i>K</i> α ₁	Mo <i>K</i> α ₁	Mo <i>K</i> α ₁	Mo <i>K</i> α ₁
Wavelength (Å)	0.70926	0.70926	0.70926	0.70926	0.70926
2θ range for lattice parameters (°)	75–80	73–78	73–78	73–78	75–80
Absorption coefficient (mm ⁻¹)	2.49	2.51	2.53	2.54	2.54
Crystal shape	Sphere	Sphere	Sphere	Sphere	Sphere
Crysta size (diameter in mm)	0.298 (2)	0.265 (2)	0.265 (2)	0.265 (2)	0.298 (2)
Data collection					
Scan type	2θ–θ	2θ–θ	2θ–θ	2θ–θ	2θ–θ
No. of reflections measured	3144	2563	2533	2525	2880
No. of independent reflections	1714	1442	1420	1395	1530
No. of observed reflections	1448	1228	1233	1257	1391
Criterion for observed reflections	<i>F</i> > 3σ(<i>F</i>)	<i>F</i> > 3σ(<i>F</i>)	<i>F</i> > 3σ(<i>F</i>)	<i>F</i> > 3σ(<i>F</i>)	<i>F</i> > 3σ(<i>F</i>)
<i>h</i>	0–10	–10–10	–10–10	–10–10	0–10
<i>k</i>	0–19	0–17	0–17	0–17	0–18
<i>l</i>	–14–14	0–13	0–13	–13–0	–13–13
2θ _{max} (°)	80	78	78	78	80
No. of standard reflections (and interval)	3 (200)	3 (200)	3 (200)	3 (200)	3 (200)
Variation of standards (%)	1	1	1	1	1
Values of extinction correction	1.72 × 10 ⁻⁵	2.04 × 10 ⁻⁵	1.97 × 10 ⁻⁵	1.91 × 10 ⁻⁵	2.00 × 10 ⁻⁵
Refinement					
<i>R</i>	0.036	0.029	0.029	0.022	0.025
<i>S</i>	0.725	0.652	0.785	0.590	0.665
No. of parameters refined	41	41	41	41	41
No. of reflections used in refinement	1429	1202	1202	1207	1369
Weighting scheme	1	1	1	1	1
(Δσ) _{max}	0.0314	–0.0385	–0.0492	–0.0303	0.0525
(Δρ) _{max} (e Å ⁻³)	1.22	0.60	0.79	0.71	0.69
(Δρ) _{min} (e Å ⁻³)	–0.97	–0.85	–1.09	–0.91	–1.06

using 25 measured reflections ($73 \leq 2\theta \leq 80^\circ$). Up to $\sin \theta/\lambda = 0.8855 \text{ \AA}^{-1}$ the intensities were measured in the 2θ – θ scan mode throughout the temperature region. Scan width is defined by $\Delta\theta = 1.3 + 0.5 \tan \theta$ and the scan speed 6° min^{-1} . Three standard reflections which were monitored every 200 reflections were observed to check the stability of measurements so that no significant variation was detected. The data were collected for two octants of the orthorhombic reciprocal space. Other experimental details and crystal data are summarized in Table 1.

Lorentz and polarization corrections were made. Absorption correction was made by numerical integration, although $\mu r \approx 0.38$ was small. Several reflections were omitted at all temperatures because these reflections seem to be affected by the superimposition of the reflections from the sapphire rod. Extinction conditions were checked upon all data at each temperature, and few unsystematic reflections to infringe the extinction conditions were measured.

The space group and setting of the crystal axes were assigned to *Pm**cn*. The structure was refined by a block-diagonal least-squares matrix on structure factor *F*, using the program AXS89 system which was rewritten

from UNICSII by Mashiyama (1991).^{*} A personal computer (NEC PC-9821 *Ap*) was used for the calculation. The function minimized in the refinement was $\sum(|F_o| - |F_c|)^2 / \sum |F_o|^2$. Atomic scattering factors for neutral atoms and anomalous dispersion corrections were taken from *International Tables for X-ray Crystallography* (1974, Vol. IV). The structure at 296 K was refined starting from the parameters at room temperature given by McGinnety (1972). Reflection data sets at the other temperatures were refined starting from the parameters at 296 K in this work. Atomic and thermal parameters were refined using reflections with $F_o > 3\sigma(F_o)$. For all reflection data sets, 19 reflections were removed because these reflections seem to be affected very strongly by the extinction effect. At the final stage of refinement an isotropic extinction correction was made (Pinnock, Taylor and Lipson, 1956). The values of the extinction coefficient are also shown in Table 1. The *R* values converged at 2.2 ~ 3.6%. The crystal structure was found to be orthorhombic, space group *Pm**cn*, at a

^{*}A list of structure factors has been deposited with the IUCr (Reference: OH0048). Copies may be obtained through The Managing Editor, International Union of Crystallography, 5 Abbey Square, Chester CH1 2HU, England.

temperature below 296 K. A final difference Fourier synthesis revealed no peak higher than $1.22 \text{ e } \text{Å}^{-3}$ throughout the temperature region investigated in this work. Other parameters are also shown in Table 1.

Results and discussion

The temperature dependence of lattice constants along the a -, b - and c -axes is shown in Fig. 1(a). Lattice constants a , b and c at 15 K contract *ca* 0.8% compared with those at room temperature. The temperature dependence of the unit-cell volume is shown in Fig. 1(b). In order to explain the temperature dependence of the unit-cell volume, we calculate the unit-cell volume $V(T)$ using the Grüneisen relation

$$V(T) = V_0 + \kappa\gamma\epsilon(\theta_D/T), \quad (1)$$

where V_0 is the value of the unit-cell volume at 0 K, κ the compressibility, and γ the Grüneisen constant (Cochran,

1973). The final term $\epsilon(\theta_D/T)$ is defined as

$$\epsilon(\theta_D/T) = 9nk_B T(T/\theta_D) \int_0^{\theta_D/T} [x^3/(e^x - 1)] dx, \quad (2)$$

where θ_D is the Debye temperature, n the number of atoms in the unit cell, and k_B Boltzmann's constant. Adams & Gibson (1931) reported $\kappa = 3.208 \times 10^{-8} \text{ Pa}$ at 293 K. Here, V_0 , γ and θ_D are fitting parameters. The Grüneisen constant γ is estimated to be 1.30. The Debye temperature and the unit-cell volume at 0 K are determined to be $\theta_D = 277 \text{ K}$ and $V_0 = 424.60 \text{ Å}^3$. The solid line in Fig. 1(b) is the calculated unit-cell volume using (1). It is seen that the temperature dependence of the unit-cell volume is well explained by the Grüneisen relation throughout the temperature region investigated in the present work. In order to explain the temperature dependence of the lattice constants, we apply the Grüneisen relation to the case of the lattice constants

$$a_j(T) = a_{0j} + A_j\epsilon(\theta_D/T), \quad (3)$$

where a_{0j} is the lattice constant at 0 K and A_j ($j = 1, 2, 3$) a proportional constant for each axis. The Debye temperature θ_D is regarded as the same value, obtained from (1), because it is a value peculiar to bulk. The lattice constant a_{0j} at 0 K and A_j are determined to be $a_{01} = 5.7224$, $a_{02} = 9.9985$, $a_{03} = 7.4211 \text{ Å}$ and $A_1 = 2.0397 \times 10^7$, $A_2 = 3.0663 \times 10^7$, $A_3 = 2.3458 \times 10^7 \text{ Å J}^{-1}$. Solid lines in Fig. 1(a) are the calculated values of each axis by (3). As the result of calculation, the temperature dependence of the lattice constants is also well explained by the Grüneisen relation. There is no anomaly for the temperature dependence of the unit-cell volume and the lattice constants.

Final atomic and anisotropic thermal parameters are listed in Table 2. Projections of the structure along the a - and c -axes at 296 and 15 K are shown in Fig. 2. The atomic parameters are satisfied with the symmetry of $Pm\bar{c}n$ throughout the temperature region. We found that the atomic parameters of K(1), K(2) and S move towards the specified directions as temperature decreases. In order to compare the α - K_2SO_4 structure with the β - K_2SO_4 structure, a common unit cell is used, *i.e.* the orthohexagonal unit cell. The orthohexagonal unit cell, with a_o , b_o , c_o , is obtained from the hexagonal basis vector a_h , b_h , c_h by $a_o = a_h$, $b_o = a_h + 2b_h$, $c_o = c_h$. Fractional atomic coordinates in the present work (x , y , z) are also transformed into $(x - \frac{1}{4}, y + \frac{1}{4}, z + \frac{1}{2})$ for K and $(x - \frac{1}{4}, \bar{y} + \frac{3}{4}, z)$ for S. Fractional atomic coordinates at high temperatures from neutron diffraction measurements (Arnold *et al.*, 1981) and those at low temperatures from the present X-ray work are shown in Table 3. The temperature dependence of the shifts of the fractional atomic coordinates Δy and Δz for K(2) in the β - K_2SO_4 structure from the atomic position in the

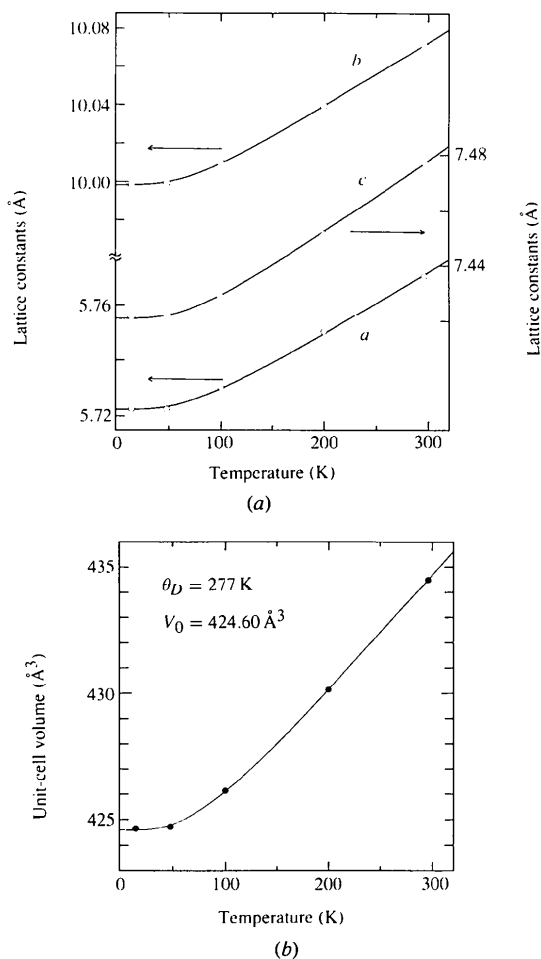


Fig. 1. Temperature dependence of (a) lattice constants a , b and c , and (b) unit-cell volume V in potassium sulfate. Solid lines are the calculated values based on the Grüneisen relation.

Table 2. Fractional atomic coordinates and anisotropic displacement parameters (\AA^2)

$$U_{eq} = (1/3) \sum_i U_{ii} a_i^* a_i^* \mathbf{a}_i \cdot \mathbf{a}_j.$$

The form of the anisotropic thermal ellipsoid is
 $\exp[-2\pi^2(h^2 a^2 U_{11} + k^2 b^2 U_{22} + l^2 c^2 U_{33} + 2hka^* b^* U_{12} + 2hla^* c^* U_{13} + 2klb^* c^* U_{23})].$

(a)						
	<i>x</i>	<i>y</i>	<i>z</i>	U_{eq}		
296 K						
K(1)	0.25	0.08935 (6)	0.17398 (7)	0.01769 (10)		
K(2)	0.25	0.79550 (5)	0.48915 (7)	0.01554 (9)		
S	0.25	0.41985 (5)	0.23295 (7)	0.00993 (9)		
O(1)	0.25	0.4162 (3)	0.0368 (3)	0.0263 (5)		
O(2)	0.25	0.5585 (2)	0.2976 (3)	0.0195 (4)		
O(3)	0.0412 (3)	0.3522 (2)	0.3017 (2)	0.0222 (3)		
200 K						
K(1)	0.25	0.08941 (4)	0.17280 (5)	0.01111 (7)		
K(2)	0.25	0.79627 (4)	0.48904 (5)	0.00964 (7)		
S	0.25	0.41993 (4)	0.23271 (6)	0.00590 (7)		
O(1)	0.25	0.4171 (2)	0.0360 (2)	0.0164 (3)		
O(2)	0.25	0.5591 (1)	0.2981 (2)	0.0123 (3)		
O(3)	0.0406 (2)	0.3520 (1)	0.3015 (2)	0.0141 (2)		
100 K						
K(1)	0.25	0.08940 (4)	0.17176 (6)	0.00595 (7)		
K(2)	0.25	0.79701 (4)	0.48888 (5)	0.00520 (7)		
S	0.25	0.41998 (5)	0.23253 (6)	0.00319 (8)		
O(1)	0.25	0.4174 (2)	0.0346 (2)	0.0094 (3)		
O(2)	0.25	0.5596 (2)	0.2986 (2)	0.0069 (3)		
O(3)	0.0394 (2)	0.3519 (1)	0.3018 (2)	0.0076 (2)		
50 K						
K(1)	0.25	0.08941 (3)	0.17138 (4)	0.00390 (5)		
K(2)	0.25	0.79729 (3)	0.48885 (4)	0.00339 (5)		
S	0.25	0.42003 (3)	0.23262 (4)	0.00208 (6)		
O(1)	0.25	0.4171 (1)	0.0342 (1)	0.0060 (2)		
O(2)	0.25	0.5601 (1)	0.2991 (2)	0.0049 (2)		
O(3)	0.0390 (1)	0.3515 (1)	0.3021 (1)	0.0052 (1)		
15 K						
K(1)	0.25	0.08942 (3)	0.17137 (4)	0.00324 (5)		
K(2)	0.25	0.79729 (3)	0.48881 (4)	0.00282 (5)		
S	0.25	0.42002 (3)	0.23263 (5)	0.00151 (6)		
O(1)	0.25	0.4170 (1)	0.0341 (2)	0.0052 (2)		
O(2)	0.25	0.5601 (1)	0.2990 (2)	0.0043 (2)		
O(3)	0.0386 (1)	0.3516 (1)	0.3020 (1)	0.0045 (1)		
(b)						
	U_{11}	U_{22}	U_{33}	U_{12}	U_{13}	U_{23}
296 K						
K(1)	0.0169 (2)	0.0197 (2)	0.0164 (2)	0	0	0.0006 (2)
K(2)	0.0185 (2)	0.0150 (1)	0.0132 (1)	0	0	-0.0005 (1)
S	0.0101 (1)	0.0095 (1)	0.0101 (1)	0	0	-0.0005 (1)
O(1)	0.0382 (11)	0.0318 (10)	0.0089 (5)	0	0	-0.0019 (7)
O(2)	0.0254 (8)	0.0120 (6)	0.0210 (7)	0	0	-0.0044 (5)
O(3)	0.0140 (4)	0.0227 (5)	0.0298 (6)	-0.0063 (4)	0.0032 (5)	0.0052 (5)
200 K						
K(1)	0.0106 (1)	0.0123 (1)	0.0104 (1)	0	0	0.0008 (1)
K(2)	0.0117 (1)	0.0089 (1)	0.0082 (1)	0	0	-0.0001 (1)
S	0.0059 (1)	0.0056 (1)	0.0061 (1)	0	0	-0.0001 (1)
O(1)	0.0245 (7)	0.0189 (6)	0.0057 (4)	0	0	-0.0010 (5)
O(2)	0.0166 (6)	0.0065 (4)	0.0138 (5)	0	0	-0.0035 (4)
O(3)	0.0090 (3)	0.0146 (4)	0.0186 (4)	-0.00042 (3)	0.0021 (3)	0.0037 (3)
100 K						
K(1)	0.0060 (1)	0.0066 (1)	0.0053 (1)	0	0	0.0005 (1)
K(2)	0.0066 (1)	0.0049 (1)	0.0041 (1)	0	0	0.0001 (1)
S	0.0037 (1)	0.0030 (1)	0.0028 (1)	0	0	0.0000 (1)
O(1)	0.0148 (6)	0.0112 (5)	0.0023 (4)	0	0	0.0001 (5)
O(2)	0.0105 (5)	0.0033 (4)	0.0070 (5)	0	0	-0.0019 (4)
O(3)	0.0050 (3)	0.0082 (3)	0.0096 (4)	-0.0025 (3)	0.0008 (3)	0.0020 (3)
50 K						
K(1)	0.0038 (1)	0.0043 (1)	0.0036 (1)	0	0	0.0002 (1)

Table 2 (cont.)

(b)	U_{11}	U_{22}	U_{33}	U_{12}	U_{13}	U_{23}
K(2)	0.0041 (1)	0.0033 (1)	0.0028 (1)	0	0	0.0000 (1)
S	0.0021 (1)	0.0020 (1)	0.0021 (1)	0	0	0.0000 (1)
O(1)	0.0088 (4)	0.0077 (4)	0.0015 (3)	0	0	0.0004 (3)
O(2)	0.0062 (4)	0.0029 (3)	0.0055 (3)	0	0	-0.0012 (3)
O(3)	0.0034 (2)	0.0059 (2)	0.0062 (2)	-0.0018 (2)	0.0009 (2)	0.0013 (2)
15 K						
K(1)	0.00337 (9)	0.00338 (8)	0.00297 (8)	0	0	0.00017 (8)
K(2)	0.00372 (9)	0.00259 (8)	0.00214 (8)	0	0	-0.00004 (7)
S	0.00193 (10)	0.00124 (9)	0.00137 (9)	0	0	-0.00010 (9)
O(1)	0.0080 (4)	0.0065 (4)	0.0012 (3)	0	0	0.0006 (3)
O(2)	0.0063 (4)	0.0022 (3)	0.0044 (3)	0	0	-0.0011 (3)
O(3)	0.0030 (2)	0.0052 (2)	0.0055 (2)	-0.0016 (2)	0.0011 (2)	0.0011 (2)

α -K₂SO₄ structure is shown in Fig. 3. Here $(\Delta x, \Delta y, \Delta z)$ is defined as

$$(\Delta x, \Delta y, \Delta z) = (x, y, z) - (x, y, z)_\alpha. \quad (4)$$

Both Δy and Δz show discontinuous changes at T_c , gradual changes below room temperature, and saturate around 0 K. As temperature increases, the atomic positions of K(1), K(2) and S approach $(0, \frac{1}{3}, \frac{3}{4})$, $(0, 0, 0)$ and $(0, \frac{1}{3}, \frac{1}{4})$, respectively, which are the special positions in the orthohexagonal unit cell. Miyake *et al.* (1980) have reported that close to the phase transition temperature, SO₄ tetrahedra jump from one state to another, and an order parameter is the orientation probability of SO₄ tetrahedra. In the high-temperature phase, S is located on a mirror plane normal to the *c*-axis. Therefore, the shift

of the S atom from the special position in the α -K₂SO₄ structure is concerned with the order parameter and the shift of K is related to a change in the configuration of neighboring SO₄ tetrahedra. It is noted that although the order parameter is almost equal to one below room temperature, the shifts of these atoms gradually increase as temperature decreases down to 15 K.

The SO₄ tetrahedron is almost regular throughout the temperature region investigated in the present work. The temperature dependence of interatomic distances and angles is listed in Table 4. The S—O bond lengths in SO₄ tetrahedra were corrected by thermal motion, using the rigid-body vibration model for SO₄ tetrahedra (Cruickshank, 1956*a,b*). We conclude that the S—O bond lengths in SO₄ tetrahedra do not change as temper-

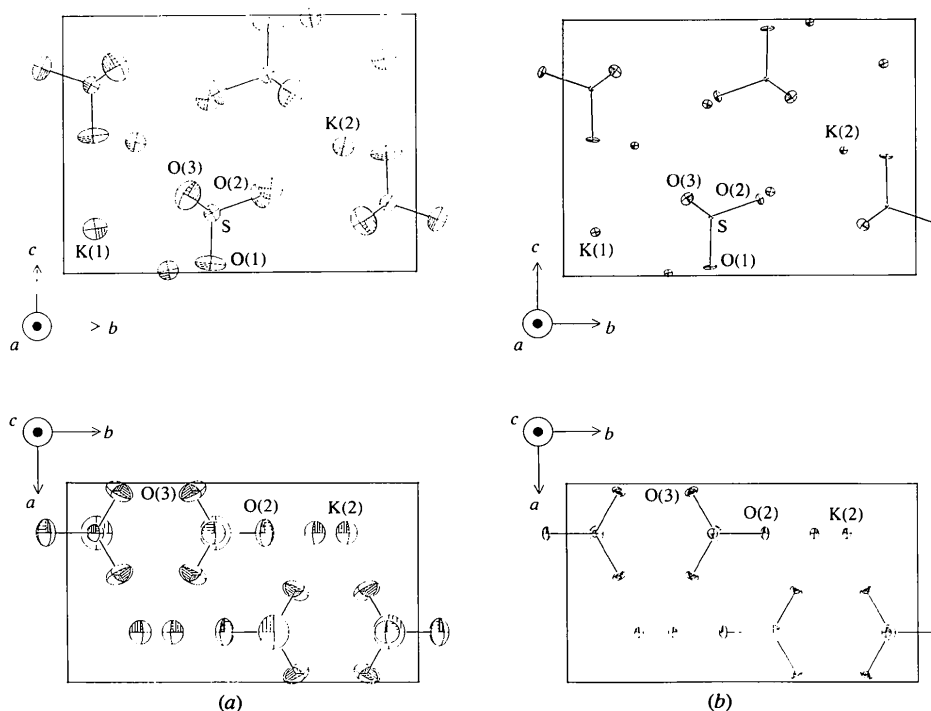


Fig. 2. Projection of the structure of potassium sulfate along the *a*- and *c*-axes at (a) 296 and (b) 15 K. Atoms are represented by 90% probability ellipsoids.

Table 3. Comparison between the fractional atomic coordinates of β -K₂SO₄ and those of α -K₂SO₄

	15 K	50 K	100 K	200 K	296 K	832 K*	847 K*	913 K*
	β -K ₂ SO ₄				α -K ₂ SO ₄			
K(1)	x	0	0	0	0	0	0	0
	y	0.33942 (3)	0.33941 (3)	0.33940 (4)	0.33941 (4)	0.33935 (6)	0.3362 (7)	1/3
	z	0.67137 (4)	0.67138 (4)	0.67176 (6)	0.67280 (5)	0.67398 (7)	0.6920 (11)	3/4
K(2)	x	0	0	0	0	0	0	0
	y	0.04729 (3)	0.04729 (3)	0.04701 (4)	0.04627 (4)	0.04550 (5)	0.0364 (5)	0
	z	-0.01119 (4)	-0.01115 (4)	-0.01112 (5)	-0.01096 (5)	-0.01085 (7)	-0.0081 (9)	0
S	x	0	0	0	0	0	0	0
	y	0.32998 (3)	0.32997 (3)	0.33002 (5)	0.33007 (4)	0.33015 (5)	0.3322 (7)	1/3
	z	0.23263 (5)	0.23262 (4)	0.23253 (6)	0.23271 (6)	0.23295 (7)	0.2401 (10)	1/4

* Data from Arnold *et al.* (1981).

ature changes. Interatomic distances S—K(*i*) decrease as temperature decreases. The angle O(*i*)—S—O(*j*) ranges from 108.68 to 110.55° at 15 K (109.47° for the regular tetrahedra).

As shown in Figs. 2(a) and (b), the thermal vibration of O(1) is very anisotropic compared with those of O(2) and O(3). The thermal ellipsoid of O(1) becomes flatter as temperature decreases. It is noted in Table 2 that the off-diagonal component U_{23} in O(1) gradually increases as temperature decreases. As seen in the projection along the *a*-axis in Fig. 2, the thermal ellipsoid of O(1) rotates around the *a*-axis in an anticlockwise direction as temperature decreases.

The mean square amplitude $\langle u_j^2 \rangle$ of vibration of atom *j* is evaluated as an equivalent isotropic thermal factor U_{eq} , as shown in Table 2. The temperature dependence of $\langle u_j^2 \rangle$ for S, K(2) and O(2) is shown in Fig. 4. Mean square amplitudes $\langle u_j^2 \rangle$ for S, K(2) and O(2) decrease monotonously as temperature decreases. The S atom has the smallest vibration among all atoms, because the S atom is located in the center of the SO₄ tetrahedron and the vibration of the S atom is restricted by surrounding O atoms. The temperature dependence of the mean square amplitude $\langle u_j^2 \rangle$ is given by

$$u_j^2 = B_j \coth[C_j/(2k_B T)], \quad (5)$$

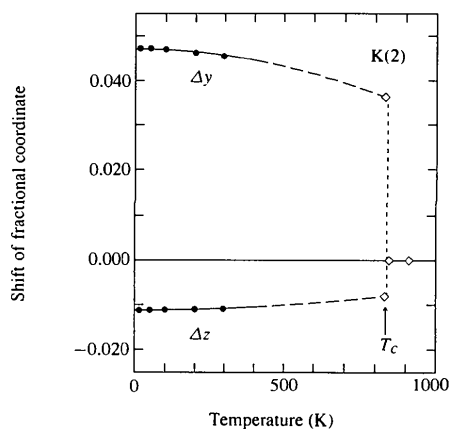


Fig. 3. Temperature dependence of shifts Δy and Δz of the K(2) atom along the *b*- and *c*-axis in β -K₂SO₄ from the position in α -K₂SO₄. (●) present work; (○) neutron diffraction by Arnold *et al.* (1981).

Table 4. Interatomic distances (Å) and angles (°)

Bond lengths of S—O in SO₄ tetrahedra have been corrected by thermal motion. Interatomic distances of S—K are the shortest. O(3') corresponds to the atom obtained from O(3) atom by the mirror plane at $x = 0.25$.

		S—O(1)	S—O(2)	S—O(3)	
296 K	Uncorrected	1.467 (2)	1.478 (2)	1.477 (2)	
	Corrected	1.475	1.485	1.484	
200 K	Uncorrected	1.466 (2)	1.480 (2)	1.476 (1)	
	Corrected	1.472	1.485	1.481	
100 K	Uncorrected	1.471 (2)	1.481 (2)	1.478 (1)	
	Corrected	1.475	1.485	1.482	
50 K	Uncorrected	1.473 (1)	1.485 (1)	1.481 (1)	
	Corrected	1.476	1.487	1.484	
15 K	Uncorrected	1.474 (1)	1.485 (1)	1.482 (1)	
	Corrected	1.476	1.487	1.485	
		S—K(1)	S—K(2)		
296 K		3.2991 (8)	3.5568 (4)		
200 K		3.2806 (7)	3.5409 (4)		
100 K		3.2644 (7)	3.5256 (4)		
50 K		3.2581 (5)	3.5207 (3)		
15 K		3.2576 (5)	2.5205 (3)		
		O(1)—O(2)	O(1)—O(3)	O(2)—O(3)	O(3)—O(3')
296 K		2.420 (3)	2.407 (2)	2.402 (2)	2.410 (2)
200 K		2.419 (2)	2.407 (2)	2.403 (2)	2.409 (2)
100 K		2.424 (2)	2.414 (2)	2.405 (2)	2.414 (2)
50 K		2.431 (2)	2.417 (1)	2.410 (1)	2.415 (1)
15 K		2.431 (2)	2.418 (1)	2.410 (1)	2.419 (1)
		O(1)—S—O(2)	O(1)—S—O(3)	O(2)—S—O(3)	O(3)—S—O(3')
296 K		110.55 (6)	109.67 (5)	108.79 (4)	109.35 (5)
200 K		110.37 (5)	109.75 (3)	108.79 (3)	109.35 (4)
100 K		110.36 (5)	109.85 (3)	108.66 (3)	109.43 (4)
50 K		110.54 (3)	109.81 (2)	108.70 (2)	109.26 (3)
15 K		110.55 (3)	109.74 (3)	108.68 (2)	109.41 (3)

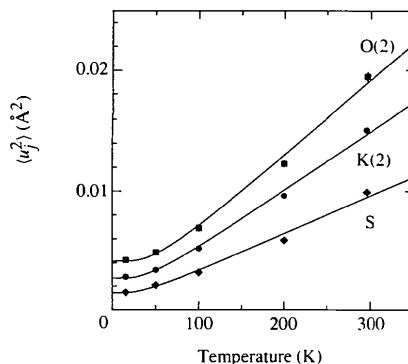


Fig. 4. Temperature dependence of mean square amplitude $\langle u_j^2 \rangle$. Solid lines are the calculated values from (5).

where B_j and C_j are constant (Noda, Kasatani, Watanabe & Terauchi, 1992). B_j for S, K(2) and O(2) is calculated, $B_S = 1.446 \times 10^{-3}$, $B_K = 2.709 \times 10^{-3}$, $B_O = 4.142 \times 10^{-3} \text{ \AA}^2$ and also C_j for these atoms, $C_S = 6.272 \times 10^{-22}$, $C_K = 7.593 \times 10^{-22}$, $C_O = 9.087 \times 10^{-22} \text{ J}$. The solid lines in Fig. 4 are the calculated values from (5). The mean square amplitude $\langle u_j^2 \rangle$ at 0 K refers to the zero-point motion. The temperature dependence of the mean square amplitude $\langle u_j^2 \rangle$ is explained by (5) throughout the temperature region investigated in the present work. No anomaly is seen for the temperature dependence of the mean square amplitude $\langle u_j^2 \rangle$.

Concluding remarks

The crystal structure of potassium sulfate was investigated at temperatures from 296 down to 15 K, using a four-circle diffractometer. Throughout the temperature region investigated in the present work, the crystal structure is found to be orthorhombic, space group *Pmcn*. Unit-cell volume and lattice constants decrease monotonously as temperature decreases. The temperature dependence of the unit-cell volume and the lattice constants is explained by the Grüneisen relation. Atomic positions of K(1), K(2) and S move to the special position of the α -K₂SO₄ structure as temperature increases. The S—O bond lengths in SO₄ tetrahedra do not alter as temperature changes. The temperature dependence of mean square amplitude $\langle u_j^2 \rangle$ decreases monotonously as temperature decreases and is explained by (5). Both

the unit-cell volume and the mean square amplitude $\langle u_j^2 \rangle$ show no anomaly to indicate a phase transition below room temperature.

The authors thank Mr Y. Kitamura for the growth of single crystals. We are also indebted to Professor H. Mashiyama at Yamaguchi University for his kind offer of the program AXS89 system.

References

- ADAMS, L. H. & GIBSON, U. R. E. (1931). *J. Wash. Acad.* **21**, 381–390.
 ARNOLD, H., KURTZ, W., RICHTER-ZINNIUS, A., BETHKE, J. & HEGER, G. (1981). *Acta Cryst.* **B37**, 1643–1651.
 BERG, A. J. VAN DEN & TUINSTRRA, F. (1978). *Acta Cryst.* **B34**, 3177–3181.
 COCHRAN, W. (1973). *The Dynamics of Atoms in Crystals*. London: Edward Arnold Ltd.
 CRUICKSHANK, D. W. J. (1956a). *Acta Cryst.* **9**, 754–756.
 CRUICKSHANK, D. W. J. (1956b). *Acta Cryst.* **9**, 757–758.
 EL-KABBANY, F. A. I. (1980). *Phys. Status Solidi A*, **58**, 373–378.
 GESI, K., TOMINAGA, Y. & URABE, H. (1982). *Ferroelectr. Lett.* **44**, 71–75.
 HASEBE, K., MASHIYAMA, H., TANISAKI, S. & GESI, K. (1984). *J. Phys. Soc. Jpn.* **53**, 1866–1868.
 IZUMI, M., AXE, J. D. & SHIRANE, G. (1977). *Phys. Rev. B*, **15**, 4392–4411.
 MASHIYAMA, H. (1991). *J. Phys. Soc. Jpn.* **60**, 180–187.
 MCGINNETY, J. A. (1972). *Acta Cryst.* **B28**, 2845–2852.
 MIYAKE, M., MORIKAWA, H. & IWAI, S. (1980). *Acta Cryst.* **B36**, 532–536.
 NODA, Y., KASATANI, H., WATANABE, Y. & TERAUCHI, H. (1992). *J. Phys. Soc. Jpn.* **61**, 905–915.
 PINNOCK, P. R., TAYLOR, C. A. & LIPSON, H. (1956). *Acta Cryst.* **9**, 173–178.
 ROBINSON, M. T. (1958). *J. Phys. Chem.* **62**, 925–928.
 SAWADA, A., TANAKA, K., MATSUMOTO, H. & NISHIHATA, Y. (1995). *Ferroelectrics*. To be published.
 UNRUH, H. G. (1970). *Solid State Commun.* **8**, 1951–1954.

Acta Cryst. (1995). **B51**, 293–300

Two 9,10-Anthracenocryptand Silver(I) Nitrate Complexes. Fluorescence Modulated by Ag⁺ as a Function of the Geometry of the Complex

BY H. ANDRIANATOANDRO, Y. BARRANS AND P. MARSAU

Laboratoire de cristallographie et Physique cristalline, URA 144 CNRS, Université de Bordeaux I, 33405 Talence CEDEX, France

AND J. P. DESVERGNE, F. FAGES AND H. BOUAS-LAURENT

Laboratoire de Photophysique et Photochimie Moléculaire, URA 348 CNRS, Université de Bordeaux I, 33405 Talence CEDEX, France

(Received 17 January 1994; accepted 12 October 1994)

Abstract

The two anthracenocryptands 3,12-octano-3,12-diaza-6,9,31,34-tetraoxa[14](9,10)anthracenophane, C₃₀H₄₀N₂O₄ (A₂₂), and 4,13-octano-4,13-diaza-7,10,33,36-tetraoxa[6](9,10)anthracenophane,

C₃₂H₄₄N₂O₄ (A₃₃), were designed to direct interactions between π -electrons and Ag⁺. In each complex displaying 1:1 stoichiometry, Ag⁺ is encapsulated in the cavity of the cryptand and coordinated to O and N atoms of the diaza-crown ether. In (A₂₂)/Ag⁺ complex (I), Ag⁺ lies at a Ag⁺–anthracene mean plane distance of 3.01 Å. Two